Defective Temporal Window of the Foveal Visual Processing in High Myopia

Haiyan Zheng,[1] Xiaoxiao Ying,[1] Xianghang He,[2] Jia Qu,[1] and Fang Hou[1]

[1]School of Ophthalmology & Optometry and Eye Hospital, Wenzhou Medical University, Wenzhou, Zhejiang, China
[2]Fuzhou Aier Eye Hospital, Fuzhou, Fujian, China

Correspondence: Jia Qu, 270 Xue Yuan Xi Road, Room 1707 Building #2, Wenzhou, Zhejiang 325027, China;
jia.qu@163.com.
Fang Hou, 270 Xue Yuan Xi Road, Room 1707 Building #2, Wenzhou, Zhejiang 325027, China;
houf@mail.eye.ac.cn.

Received: December 7, 2020
Accepted: June 5, 2021
Published: July 8, 2021

Citation: Zheng H, Ying X, He X, Qu J, Hou F. Defective temporal window of the foveal visual processing in high myopia. *Invest Ophthalmol Vis Sci.* 2021;62(9):11. https://doi.org/10.1167/iovs.62.9.11

Purpose. To investigate the temporal characteristics of visual processing at the fovea and the periphery in high myopia.

Methods. Eighteen low (LM, ≤ -0.50 and > -6.00 D) and 18 high myopic (HM, ≤ -6.00 D) participants took part in this study. The contrast thresholds in an orientation discrimination task under various stimulus onset asynchrony (SOA) masking conditions were measured at the fovea and a more peripheral area (7°) for the two groups. An elaborated perceptual template model (ePTM) was fit to the behavioral data for each participant.

Results. An analysis of variance with three factors (SOA, degree of myopia and eccentricity) was performed on the threshold data. The interaction between SOA and degree of myopia in the fovea was significant ($F(4, 128) = 2.66$, $P = 0.036$), suggesting that the masking effect had different temporal patterns between the two groups. The temporal profiles for the two groups were derived based on the ePTM model. The peak and the spread of the temporal window in the fovea were much lower and wider, respectively, in the HM group than that in the LM group (both Ps < 0.05). There was no significant difference in the peripheral temporal window between the two groups.

Conclusions. High myopia is associated with defective temporal processing in the fovea, captured by a flattened temporal window.

Keywords: eccentricity, external noise, high myopia, perceptual template model, temporal processing

Myopia, a common refractive error primarily caused by excessive axial elongation of the vitreous chamber, is one of the most prevalent eye diseases worldwide, especially in Asia.[1–3] With the significant increase in prevalence, Holden et al.[1] predicted that by 2050 myopia will affect nearly 48 billion people (49.8% of the world population). The visual impairments of myopia can be mostly corrected with spectacles, contact lenses, or refractive surgery. However, high myopia, characterized by more exaggerated axial elongation and thinning of the sclera,[4] is usually accompanied by a variety of abnormal functional and structural changes.[5–10]

The spatial aspects of visual deficits in high myopia have been demostrated in many studies.[6,9,11–16] Living in a dynamic environment requires our visual system to process visual information over extended intervals of time to maintain a stable and reliable performance.[17–20] It has been reported recently that myopes showed significantly reduced performance when viewing dynamic stimuli.[21–23] However, the temporal properties of visual information processing in high myopia have not received as much attention as spatial processing and are still not well understood.

Kuo et al.[22] found that the minimum displacement detection threshold (Dmin) for random dot stimuli was 25% higher in high myopes (spherical equivalent refraction < -5.00 D) than in emmetropes. More importantly, Dmin correlated well with refractive error and axial length over a wide range of myopia. Simlarly, the disparity threshold for flickering stimuli at 4 Hz was negatively correlated with refractive error.[23] On the basis of these results, we might infer that high myopes may suffer difficulties when processing dynamic information. However, using a backward masking paradigm,[24,25] Kuo et al.[21] reported that although myopes showed significantly decreased performance under the masking condition compared with emmetropes, there was no significant difference in performance between low and high myopes (although they noticed a trend for an effect of magnitude of myopia on task performance).

A possible reason why Kuo et al.[21] did not find any statistically significant difference between low and high myopia might be the large individual differences in visual performance within each group. Although individual performance in the no-mask condition was treated as a covariate in their analysis,[21] including covariates is not as statistically powerful as controlling the variable directly.[26] Thus a strict control of spatial vision could help differentiate possible temporal differences between low and high myopia. On the other hand, there was one interesting finding worth noting in the backward masking study of Kuo et al.[21] By performing an analysis of variance (ANOVA) on the location masking data, Kuo et al.[21] found there was a significant interaction between myopia group and stimulus onset asynchrony (SOA). This

result indicated that performance changes as a function of SOA were different between groups. Given that performance in the no-masking condition varied a lot among subjects, in this article, we focus on the shape of the performance curve in the temporal domain instead of absolute performance at a single time point to make an informative comparison between low and high myopic groups. To complete this analysis, we directly estimate and compare the full temporal characteristics of visual processing.

We also examine temporal visual processing in the periphery for high myopia. Although Chui et al.[5] reported that with increased refractive error, the retina stretching was locally uniform over the central ±15° of visual field, the extent of the impairmens in myopia has been found to be uneven across the visual field in other studies. Using multifocal electroretinograms, Kawabata and Adachi-Usami[15] found that the amplitude reduction between the central region and the peripheral annuli (up to 25° horizontal or 20° vertical from the center) was greater in the high myopic group than in the emmetropic/low myopic group. There are also significant differences in the intraretinal layer thicknesses in the peripheral region (an anulus between 1.5 mm and 3 mm radius circles concentric at the fovea) of high myopic eyes.[27] It is therefore interesting to examine whether the temporal characteristics in high myopia would differ between the fovea and the periphery.

Taken together, in the study reported here, we aimed to investigate the temporal characteristics of visual information processing at the central and more peripheral visual fields in low and high myopia. We measured the contrast thresholds of an orientation discrimination task with white external noise masks under different target-mask SOA conditions. By presenting the noise masks at different SOAs, the temporal dynamics of visual information processing can be mapped. This paradigm has been previously used to investigate the temporal profile under the effects of attention[28] and aging.[29] Both central (0°) and more peripheral (7°) visual fields were examined in low and high myopia. The contrast threshold in the condition without noise masks was used as the baseline performance for spatial vision. The masking effects under different SOA conditions were anlyzed, and an elaborated perceptual template model (ePTM)[28] was fit to the trial-by-trial data. The temporal profiles of visual processing at the two eccentricities derived from the best-fitting ePTM were compared between the two groups.

Material and Methods

Participants

Thirty-six students from Wenzhou Medical University participated in the study. All participants underwent general ophthalmic and refractive examinations. They all had normal or corrected-to-normal vision (≤0.0 log MAR, ETDRS chart), astigmatism of less than 1.50 diopter in both eyes, and anisometropia of less than 1.50 D. Some highly myopic participants exhibited fundus tessellation. Participants with pathologic complications were excluded. None of the participants had history of refractive surgery, trauma, or systemic diseases.

Participants were assigned to one of two groups comprising low myopes (LM) and high myopes (HM), based on their spherical equivalent refraction (SEQ). There were 18 participants in the LM group (≤−0.50 and >−6.00 D; mean ± SD SEQ: −2.09 ± 1.12 D; SEQ range: −4.25 ∼ −0.75 D; mean ± SD age: 25.0 ± 2.57 years; 10 females) and 18 participants in the HM group (≤−6.00 D; −7.65 ± 1.23 D; −10.00 ∼ −6.25 D; 25.3 ± 2.63 years old; 12 females). Participants wore the best optical corrections for the test distance during the experiment.

The research was approved by the ethical committee of Eye Hospital affiliated to Wenzhou Medical University and adhered to the tenets of the Declaration of Helsinki. Written informed consent was obtained from each participant before the experiment. All but one participant (first author, H.Z., HM group) were naive to the purpose of the study.

Apparatus

The experiment was conducted in a dimly lit room. Custom programs written in MATLAB (MathWorks Corp., Natick, MA, USA) with Psychtoolbox extensions[30] were used in the experiment and run on a DELL OptiPlex 7050 computer (Dell Inc., Landerock, TX, USA). Stimuli were displayed on a gamma-corrected Asus flat panel monitor (PG278QR; Asus Corp., Taipei, Taiwan). The display had a spatial resolution of 2560 × 1440 pixels, a refresh rate of 120 Hz and a mean luminance of 70.4 cd/m^2. Each pixel subtended 0.02° at the viewing distance of 0.668 m. A chin rest was used to minimize head movement during the experiment. The participants viewed the stimuli monocularly using their dominant eye with best optical correction as appropriate. Eye dominance was determined by the hole-in-card test[31] for each participant. The eye not being tested was occluded by an opaque patch. Eye fixations were monitored by a desktop mount video-based eye tracker (Eyelink 1000 Plus; SR Research Ltd., Mississauga, Ontario, Canada) to make sure that the stimuli were presented to the required retinal locations throughout the experiment.

Stimuli

The orientation discrimination task used Gabor stimuli oriented ±45° from vertical. The spatial frequency and spatial constant (standard deviation [SD]) of the Gabor stimuli were 1.0 cycle per degree (c/°) and 1.0°, respectively. The external noise images had a size of 200 × 200 pixels and consisted of 40 × 40 square noise elements. The normalized luminance of each noise element of every external noise image was independently sampled from a Gaussian distribution with a mean of 0.5 and a standard deviation of 0.16. The Gabor signal and external noise frames were presented at the same location, either the center or 7° from the center of the screen (supratemporal field; 45° meridian) depending on the testing location (Fig. 1a). This eccentricity was determined based on the results of the pilot study. As the contrast threshold increased significantly with eccentricity, 7° from the center was the most eccentric location where the contrast threshold could be reliably measured.

The stimulus in each trial consisted of 17 successive image frames and lasted 283.3 ms. The ninth image frame was the Gabor signal. There were five masking conditions in the experiment according to their SOA: SOA 16.7 ms, 33.3 ms, 50.0 ms, 83.3 ms, and SOA ∞ (no noise mask) (Fig. 1b).[28] The noise masks were presented at ±1, ±2, ±3 & 4, and ±5, 6, 7 & 8 frame positions relative to the signal (at frame 0) in SOA 16.7 ms, 33.3 ms, 50.0 ms, and 83.3 ms conditions, respectively. The symmetrical noise masks were used to estimate the joint effects of both the forward and backward masking.

Investigative Ophthalmology & Visual Science

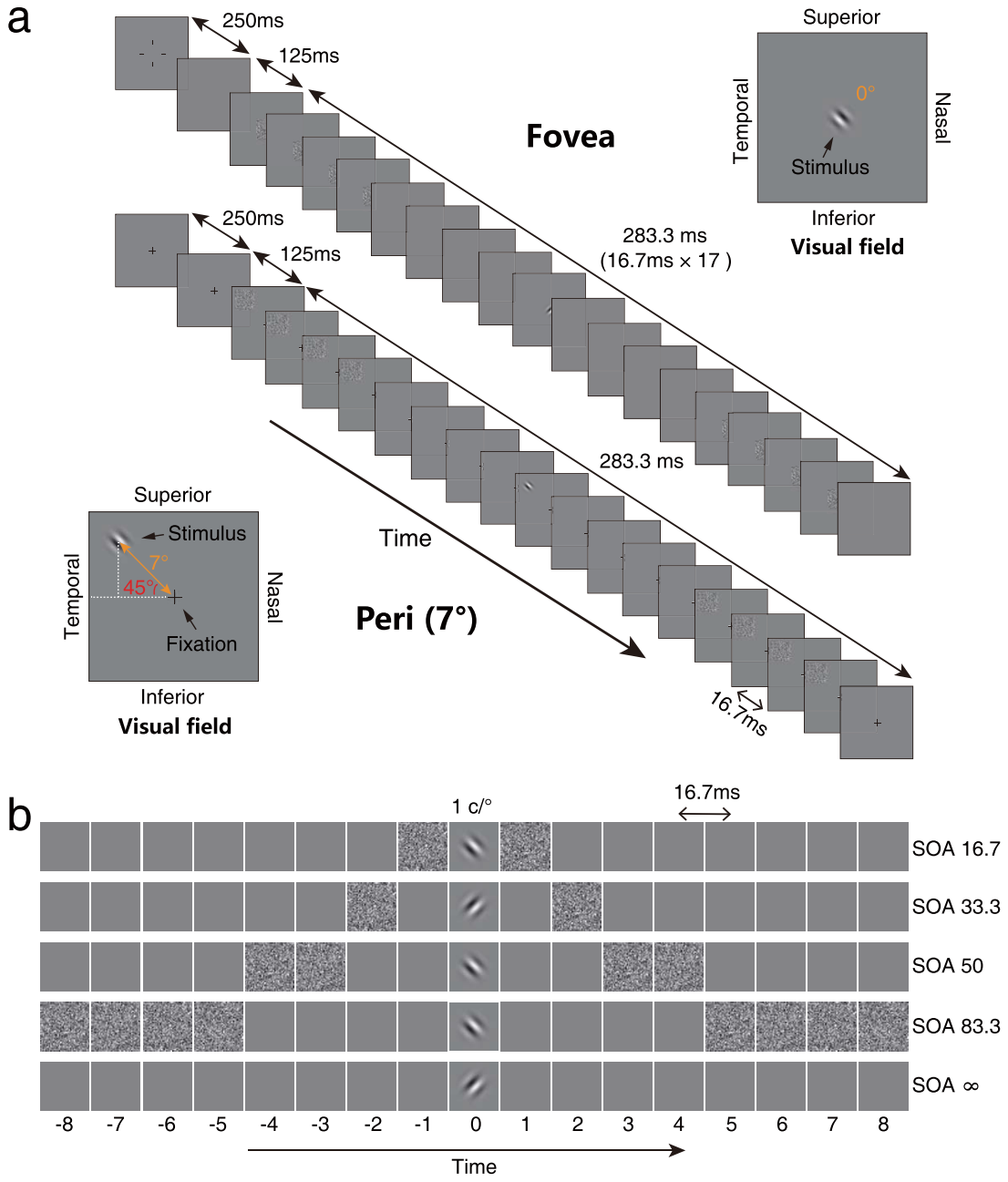

Figure 1. Illustrations of the paradigm. **(a)** Image sequence of stimuli in the foveal and peripheral (7°) conditions. **(b)** Five external noise configurations used in the current study. The noise masks were presented at ±1, ±2, ±3 & 4, and ±5, 6, 7, & 8 frame positions relatively to the signal (at frame 0) in conditions SOA 16.7 ms, SOA 33.3 ms, SOA 50 ms, and SOA 83.3 ms. The no-noise condition was noted as SOA ∞.

Because the temporal curve of the masking effect changes rapidly at short SOA and slowly at long SOA,[24] the noise mask had a shorter duration for conditions SOA 16.7 ms and 33.4 ms, and a longer duration for conditions SOA 50 ms and 83.4 ms. This allowed us to use five temporal conditions to cover the whole temporal range of "integration masking" (SOA ± 150 ms)[32–34] without sacrificing precision in a single test. The shorter noise duration at short SOA conditions could keep the threshold within the measurable range (<1.0), whereas the average temporal weight over multiple noise frames could still provide good approximation of the "true" temporal profile at long SOA conditions.

Design

Each participant completed the fovea and periphery tests in two separate sessions. The order of tests was counterbalanced across participants. There were five noise conditions in each test session. The trials of different conditions were interleaved randomly. The Psi method[35] was used to measure the monocular contrast thresholds in each condition.

The eye fixation was monitored in each trial. When the gaze deviated more than 1.5° from the center of the screen or eye blinked during stimulus presentation, a warning message "Fail" appeared and the trial was repeated later

Investigative Ophthalmology & Visual Science

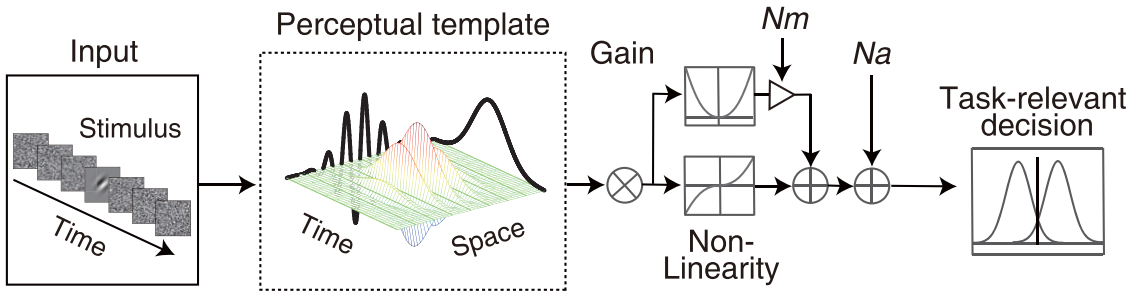

Figure 2. Illustration of the ePTM model. It consists of five major components: a perceptual template, a nonlinear transducer function, a multiplicative internal noise source *Nm*, an additive internal noise source *Na*, and a decision process.

in the test session to guarantee there were 100 effective trials tested in each noise condition. The participants were encouraged to take breaks after each 100-trial block. Each test session lasted about an hour.

Procedure

Before each test session started, the participants were given at least five minutes to adapt to the dim test environment and a practice session of about 100 trials to ensure they fully understood the task. At the beginning of each block, a calibration procedure and a validation procedure, both with default settings from the eye tracker, were conducted successively to ensure the accuracy of eye position recording. Within each block, the participants were asked not to move their head.

Each trial began with a brief tone signaling its onset. In the foveal testing session, a crosshair fixation was then displayed for 250 ms at the center of the screen, and after a blank screen (125 ms) with background luminance, the 17-frame stimulus sequence (283.3 ms) was presented. The participants were asked to judge the orientation of the Gabor signal and respond via the computer keyboard. The screen was then kept blank until the response was received. Auditory feedback was provided after each correct response. A new trial started 500 ms after the response was made.

In the peripheral testing session, a fixation-cross was always presented at the center of the screen throughout a trial. The 17-frame stimulus sequence was presented at the eccentricity of 7° (supratemporal field; 45° meridian). The participants were asked to fixate at the center of the screen. The rest of the settings were the same as those used in the fovea testing session.

Analysis

A Weibull psychometric function was fit to the raw trial-by-trial response data in each SOA and eccentricity condition using a maximum likelihood procedure .[36] The contrast thresholds derived from the best fitting psychometric functions were used to analyze masking effects. Repeated measures ANOVA was used to analyze the effects of different factors, as well as their interactions.

To quantitatively estimate the characteristics of temporal processing, the ePTM[37] was used to fit the entire set of raw trial-by-trial response data of each individual. The ePTM, developed by Lu et al.,[28] has been used previously to investigate the temporal profile and the effects of attention[28] and aging.[29] A schematic diagram of the ePTM is shown in Figure 2. The visual input stream consists of both signal and noise, and enters the visual system through a perceptual template. The perceptual template is essentially a spatiotemporal filter with a total gain value of β to the signal relative to the external noise,[38,39] and weight W_t at different time t, which selectively processes task-relevant information and excludes task-irrelevant information. After filtering, the information goes through a nonlinear transducer, characterized by a power function with an exponent of γ, then gets contaminated by an internal additive noise source *Na* and a multiplicative noise source *Nm*. The latter noise source mimics the contrast-gain control mechanism of neurons. Finally, the noisy information is sent to the decision unit. For more details about the ePTM, please see Appendix A and elsewhere.[29,37]

In the analysis, data from two participants, one in the LM group and the other in the HM group, were excluded because their peak and full width at half maximum (FWHM) of the temporal profile exceeded ±2 SDs of the range about the mean. The data of the remaining 34 participants are presented in this article.

Results

Masking Effects

The contrast thresholds at two different eccentricities for the LM and HM groups are plotted against the noise SOA in Figures 3a and 3b. A repeated measures ANOVA was performed to test the effects of SOA, degree of myopia and eccentricity on the contrast threshold in the orientation discrimination task. There were significant effects of SOA (F (3.14, 128) = 372, Greenhouse-Geisser corrected, $P = 4.75 \times 10^{-55}$), eccentricity (F (1, 32) = 80.5, $P = 3.01 \times 10^{-10}$) and SOA × eccentricity interaction (F (4, 128) = 63.4, $P = 1.95 \times 10^{-29}$). As the SOA increased, the contrast threshold decreased. The threshold decreased more rapidly in the fovea than in the periphery. Contrast thresholds were greater in the periphery (7°) than in the fovea in the two groups (one-tailed paired t-test, all Ps < 0.05, at all SOA conditions except SOA 33.3 ms in the LM group and SOA 50 ms in the HM group).

Neither myopia degree (F (1, 32) = 0.021, P = 0.885) nor the interaction between myopia degree and eccentricity (F (1, 32) = 0.175, P = 0.678) was significant. These results indicated that there was no difference in the average performance between the two groups at either the fovea or the periphery. However, the interaction between SOA and degree of myopia was significant (F (4, 128) = 2.66, P = 0.036), which suggests that the masking effect had

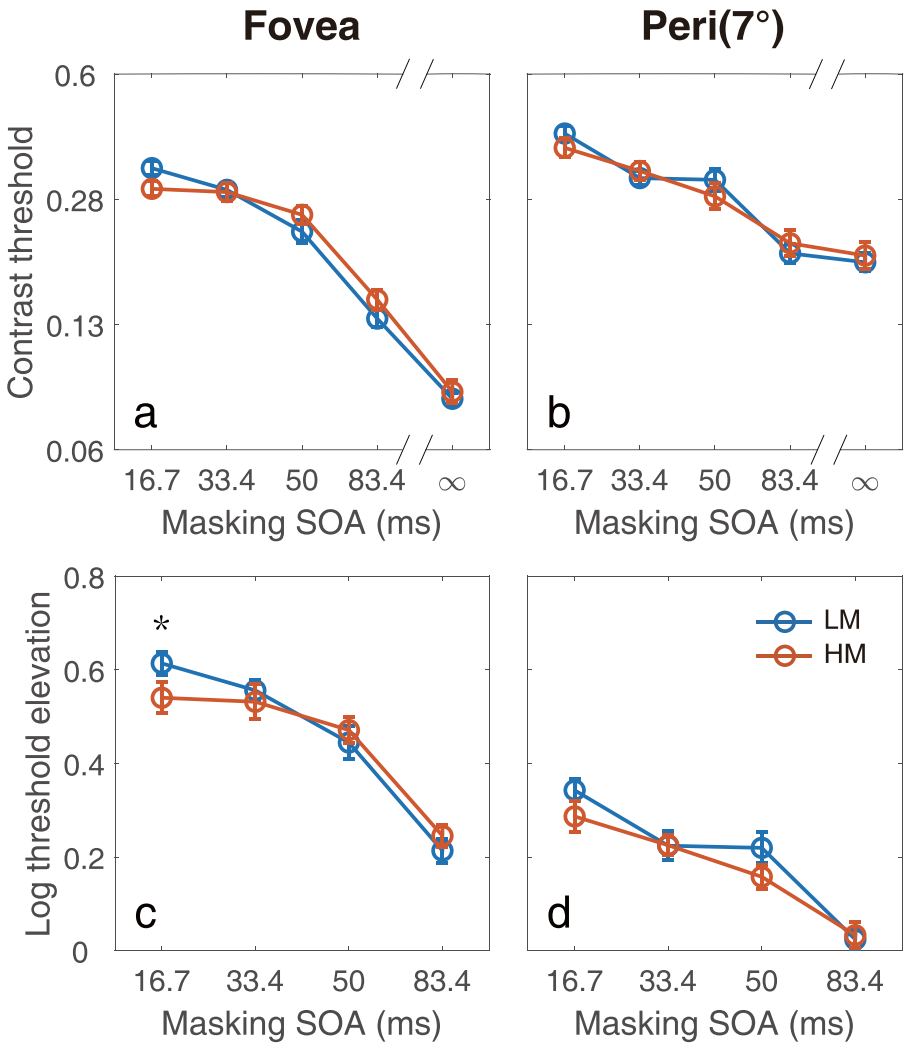

Figure 3. The top row shows the contrast thresholds of the HM and LM groups as a function of SOA in the fovea **(a)** and in the periphery **(b)**. The bottom row shows the threshold elevations of the HM and LM groups as a function of SOA in the fovea **(c)** and in the periphery **(d)**. *Blue*: the LM group; *Red*: the HM group. *Error bars*: ±1 SE. *Asterisks*: statistical significance with $P < 0.05$.

different temporal patterns across SOA between the LM and HM groups (Figs. 3a, 3b).

To better demonstrate the difference in the pattern of masking effects between the two groups, the threshold elevations (difference in log threshold between the masking and no masking conditions) were calculated and plotted in Figures 3c and 3d. Again, a repeated measures ANOVA with three factors (SOA, degree of myopia and eccentricity) was performed on the threshold elevations. Significant effects of SOA (F (3, 96) = 249, $P = 3.68 \times 10^{-45}$) and eccentricity (F (1, 32) = 143, $P = 2.46 \times 10^{-13}$) were found. The noise mask induced larger masking effects in the fovea than in the periphery (one-tailed paired t-test, all Ps < 0.05, Figs. 3c, 3d).

There was no significant difference in the threshold elevation between the LM and HM groups (F (1, 32) = 0.466, P = 0.500), but there was a significant interaction between SOA and degree of myopia (F (3, 96) = 4.07, P = 0.009). It again indicated that the masking effect across SOA had different patterns between the two groups. A post hoc analysis showed that at the fovea, the masking effect at SOA 16.7 ms was weaker in the HM group than in the LM group (one-tailed two sample t-test, t (32) = 1.79, P = 0.041). There was no significant difference in the masking effect at other SOAs between the two groups.

Model Fitting

To further investigate the temporal difference between the LM and HM groups, we characterized the temporal profile of visual processing at the central and peripheral visual field in the two myopia groups using the ePTM analysis. The ePTM was fitted to the trial-by-trial response data for each participant using a maximum likelihood procedure. The goodness of fit was determined by the χ^2 test.[36]

For all participants, the ePTM fitted the behavioral data well (all Ps > 0.05). The internal additive noise and template gain at different eccentricities in the two groups are shown in Figure 4. No statistical difference in the internal additive noise Na or the template gain β was found between the two groups in either eccentricity (two sample t-test, all Ps > 0.1). The internal additive noise was significantly lower in the fovea than that in the periphery for both LM (−3.76 ± 0.223 vs. −2.97 ± 0.178, paired t-test, t (16) = 7.76,

Investigative Ophthalmology & Visual Science

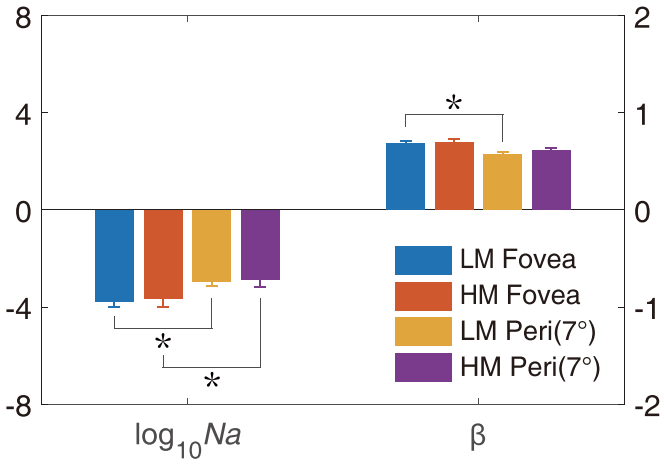

Figure 4. The internal additive noise *Na* and the template gain β of the best fitting ePTM at different eccentricities for the two groups. *Blue*: the fovea of the LM group; *Red*: the fovea of the HM group; *Yellow*: the periphery (7°) of the LM group; *Purple*: the periphery (7°) of the HM group. *Error bars*: ± 1 SE. *Asterisks*: statistical significance with $P < 0.05$.

$P = 8.18 \times 10^{-7}$) and HM (-3.67 ± 0.314 vs. -2.88 ± 0.276, paired *t*-test, t (16) = 7.36, $P = 1.60 \times 10^{-6}$) groups. In the LM group, the template gain in the fovea was significantly higher than that in the periphery (0.684 ± 0.028 vs. 0.570 ± 0.028, paired *t*-test, t (16) = 3.32, $P = 0.004$). In the HM group, there was no significant difference in β between the two retinal locations (0.697 ± 0.029 vs. 0.610 ± 0.028, paired *t*-test, t (16) = 2.05, $P = 0.057$). The multiplicative noise *Nm* and non-linearity of the transducer function γ were not significantly different between the two groups (two sample *t*-test, all *P*s > 0.1).

Temporal Window

The best fitting temporal weights (W_t) of the ePTM for the two groups in the fovea and the periphery are plotted as a function of SOA in Figure 5. As we can see, the temporal weighting functions are bell-shaped. The temporal weight decreased as the noise mask was presented further (in time) away from the onset of the target. Thus, we refer to this weighting function as the temporal window of visual processing. A repeated measures ANOVA with three factors (SOA, degree of myopia and eccentricity) was performed. As SOA increased, the weight decreased (F (2.25,96) = 807, Greenhouse-Geisser corrected, $P = 1.52 \times 10^{-51}$). The effect of myopia degree on the temporal weights was not significant (F (1,32) = 0.535, $P = 0.470$); however, the interaction between SOA and myopia degree was significant (F (3,96) = 2.78, $P = 0.045$). These results indicate that the temporal profiles of the LM and HM groups have different shapes. There was a significant effect of eccentricity (F (1,32) = 19.9, $P = 9.5 \times 10^{-5}$), and a significant interaction between SOA and eccentricity (F (3,96) = 6.51, $P = 4.68 \times 10^{-4}$), suggesting that the weight profiles were also different between different retinal locations.

In the fovea, the post hoc analysis showed that the temporal weight in the HM group was significantly lower at SOA 16.7 ms than in the LM group (one-tailed two sample t-test, t (32) = 2.44, $P = 0.010$), but was higher at SOA 83.3 ms (one-tailed two sample *t*-test, t (32) = 1.77, $P = 0.043$) than in the LM group. No significant difference in the temporal weight was found at the fovea between the two myopia groups at any other SOA conditions (two sample *t*-test, all *P*s > 0.05). In the periphery, there was no significant difference in the temporal weight between the two groups at any SOA conditions (two sample *t*-test, all *P*s > 0.05).

To quantify the shape of the temporal window, a Gaussian function, $g(t) = peak \cdot \exp(-(\frac{t^2}{2\sigma^2}))$, was used to fit the temporal weights at different SOAs. To guarantee the data derived from each configuration contributed equally to the entire fitting, the weight of each data point (W_t) to the sum of the residuals was adjusted. The peak amplitude and FWHM, computed as $2\sqrt{2\ln(2)}\sigma$) of the temporal window, were calculated at each retinal location for each participant. The average temporal windows at the fovea and periphery of the two groups are shown in Figure 5.

In the fovea, the peak amplitude was significantly lower in the HM group than in the LM group (0.446 ± 0.008 vs.

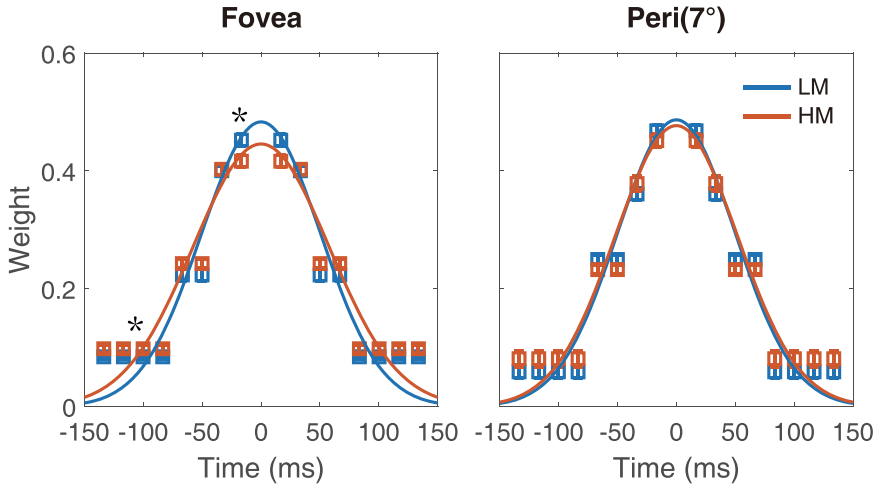

Figure 5. The temporal weights ($W_{16.7}$, $W_{33.3}$, $W_{50.0}$, and $W_{83.3}$) of the two groups in the fovea (*left*) and the periphery (*right*). The continuous curves are the best-fitting Gaussians. *Blue*: the LM group; *Red*: the HM group. *Error bar*: ±1 SE. *Asterisks*: statistical significance with $P < 0.05$.

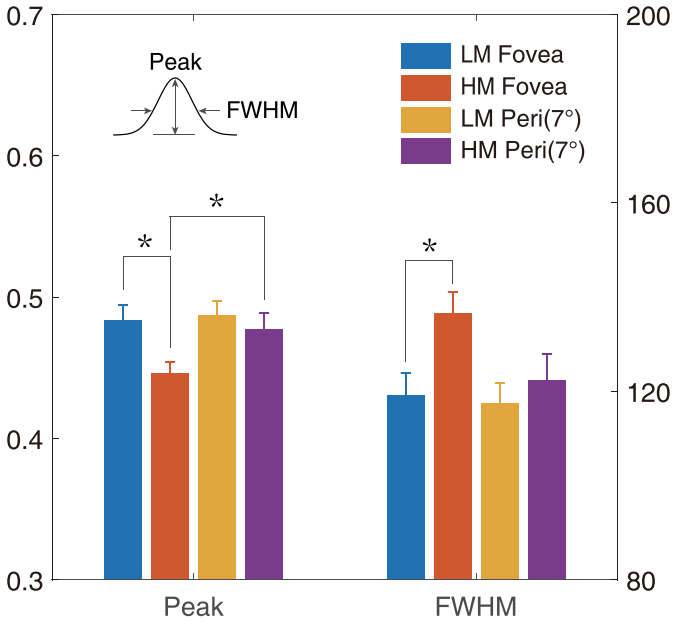

Figure 6. The peak and FWHM of the temporal window at the two eccentricities for the two groups. *Blue*: the fovea of the LM group; *Red*: the fovea of the HM group; *Yellow*: the periphery of the LM group; *Purple*: the periphery of the HM group. *Error bar*: ±1 SE. *Asterisks*: statistical significance with $P < 0.05$.

0.483 ± 0.011, two sample *t*-test, t (32) = 2.71, $P = 0.011$), and the FWHM was wider in the HM group than in the LM group (136 ± 4.49 ms vs. 119 ± 4.66 ms, two sample *t*-test, t (32) = 2.67, $P = 0.012$). Compared with the LM group, the HM group had a flatter (7.7% lower and 14.5% wider) temporal window in the fovea (Fig. 6). However, in the periphery, neither the peak amplitude nor the FWHM was significantly different between the two groups (two sample *t*-test, both *P*s > 0.1, Fig. 6).

We also compared the shape of the temporal window between the two eccentricities for each myopic group. In the LM group, no significant difference in either the peak amplitude or the FWHM between the two eccentricities was found (paired *t*-test, both *P*s > 0.1). In the HM group, the peak amplitude in the fovea was significantly lower than in the periphery (0.446 ± 0.008 vs. 0.477 ± 0.012, paired *t*-test, t (16) = 2.30, $P = 0.035$). No significant difference in the FWHM between the fovea and the periphery was found (136 ± 4.49 vs. 122 ± 5.58, paired *t*-test, t (16) = 2.08, $P = 0.054$). Taken together, the results indicate that high myopes have a defective temporal window in the fovea, not the periphery.

Discussion

In this study, we aimed to test if there was any temporal deficit in high myopes. We measured contrast thresholds in an orientation discrimination task across a variety of target-mask SOA conditions at two eccentricities for low and high myopic participants. There was no significant difference in performance between the LM and HM groups in a spatial condition without temporal noise masks for each retinal location, which indicated that the visibility of the target was similar for both LM and HM groups. This allowed us to attribute the differences revealed in the later analysis to a deficit in the temporal domain. There was a significant interaction between SOA and the degree of myopia in the fovea which suggests that the temporal pattern of the masking effect was significantly different between the LM and HM groups. With the ePTM analysis, we estimated the temporal window of visual processing in the fovea and the periphery for all participants. The HM participants showed a flattened temporal window (lower peak and wider spread) than the LM participants at the fovea. There was no difference in the peripheral temporal window between the two groups.

To some extent, our result is consistent with that reported in Kuo et al.[21] They found that myopic observers performed significantly worse than emmetropes in a location task when masks were presented after the stimuli. The difference between groups was still evident when the performance in a no mask condition (baseline) was considered. Besides the temporal deficits revealed by masking, other groups have also found differences in binocular temporal visual processing between myopic and emmetropic groups. Vera-Diaz et al.[23] found that when the stimuli were temporally modulated, binocular functions such as disparity threshold and interocular balance were different between the two groups. More myopic observers tended to have worse disparity thresholds to the flickering stimuli at 4 Hz.[23] Neither of these effects could be attributed to differences in their monocular spatiotemporal contrast sensitivity functions. Despite the differences among the three studies, these results together suggest that high myopia may be associated with multiple temporal deficits that involve different visual mechanisms, and the temporal deficit in high myopia can be independent of spatial visual processing.

One important task of our visual system is to efficiently pick up the signal-of-interest buried in the noisy spatiotemporal input. The bell-shaped temporal window estimated by the ePTM analysis reflects the relative processing efficiency function in the time domain, which represents how well the visual system is tuned to the onset of the target or, equivalently, how well it excludes external distraction.[28] The flattened temporal window at the fovea of the HM participants indicates that they are more susceptible to the disturbance

Investigative Ophthalmology & Visual Science

and less able to extract task-relevant information in the time domain than low myopic participants. Furthermore, the width of the temporal window can be regarded as the integration time within which the visual information would be grouped and interpreted as a single event. This integration time could limit the temporal processing capacity or resolution in processing successive events.[40,41] Wutz and Melcher[40] proposed that the integration of sensory information usually occurs over a brief interval of around 100 ms. Landau Ayelet and Fries[42] observed a rhythmic temporal structure in psychophysical performance with a period of approximately 125 ms. VanRullen and Koch[43] suggested that the temporal resolution of visual system in serial processing was about 10 Hz. The full width of the temporal window at the fovea of the low myopic participants found in current study (119 ms) was comparable with the time scales of visual processing reported in the aforementioned studies. The wider temporal window for the HM participants suggests a lower temporal resolution for processing successive events.

The wider temporal window in high myopia may be related to the changes in the retina. With the abnormal elongation of the globe,[4] high myopia is associated with a variety of anatomical changes in the retina,[10,44–46] which have been linked to retinal functional deficits,[5,9,44,47–50] such as the delayed mfERG responses[15,50] and decreased macular light sensitivity.[9,44] Park et al.[46] reported that the photoreceptor layer thickness in the foveola significantly decreased with increasing myopia. Similarly, Wang et al.[44] found that the thickness of the myoid and ellipsoid zone within 2° from the macular center was correlated with the axial length. The thinning of the photoreceptor retina could be associated with lower cone density.[44] However, Wang et al.[51] found the angular (sampling) cone density increased with the axial length and argued that the deficits in best-corrected foveal vision in myopes cannot be explained by increased photoreceptor spacing caused by retinal stretching. Therefore the temporal deficit observed in our HM group is possibly due to the structural and functional changes at the postreceptoral level in the retina.

On the other hand, the temporal deficits in the fovea of high myopes could also be linked to changes in downstream cortical areas, as visual pattern masking involves cortical processing.[24] It has been hypothesized that abnormal visual experience introduced by prolonged near work could cause the attentional deficit in myopia.[52] Kang et al.[53] reported that myopic defocus stimulation could significantly increase the attention-related changes in brain activity, and these attention-related changes were less significant in their myopic group than in their nonmyopic group. Other functional magnetic resonance imaging studies have reported that high myopes show cortical deficits involving attentionl control.[54,55] As corroborating evidence, it has been shown that the temporal window became wider when a spatial attention cue was absent.[28] Taken together, the temporal deficits found in the current study could also be due to an attentional deficit in high myopia.[52,54,55]

We did not observe any difference in the temporal window at the more peripheral location, between the LM and HM groups. Typically, the periphery is more sensitive to dynamic visual information input than the fovea.[56-60] Several studies have suggested that high myopic eyes show greater changes in the periphery than in the fovea.[15,27,61] For example, Liu et al.[27] found that the intraretinal layer thickness of high myopic eye varied more significantly from emmetropic controls in more peripheral regions (an annulus between 1.5 mm- and 3 mm-radius circles concentric at the fovea) than in the foveal area. Kerber et al.[62] reported that the contrast detection thresholds for targets presented in the far peripheral visual field (30° eccentricity) were impaired in the myopic participants when attention was demanded in central vision. However, other studies found no functional differences between myopic and emmetropic participants. For example, Macedo et al.[63] found that myopes and emmetropes showed similar normal temporal integration in different retinal locations (10°, 20°, and 30° in the temporal and nasal retina).

The current study has several limitations. First, myopia was classified by refractive error in the absence of axial length data. Ideally, axial length should be measured to provide information about the amount of excessive axial elongation in high myopia. Second, there was no overlap in the SEQ values of high and low myopic participants. Therefore the relationship between the temporal window and the myopia degree could not be fully explored. Last, emmetropes were not included in our study. This might have led to an apparent underestimation of the observed temporal deficit in the HM group.

In summary, the current study revealed a temporal processing deficit in the fovea of high myopes. Specifically, they showed a flattened, albeit widened temporal window in their fovea, compared to low myopes. The impact of this deficit on daily visual functions represents an interesting question to address in future studies.

Acknowledgments

The authors thank the two anonymous reviewers and the EBM for their helpful comments and suggestions, and thank Peter Bex for proofreading the manuscript.

Supported by the Department of Human Resources and Social Security of Zhejiang Province (Qianjiang Talent Project, QJD1803028 to FH), Zhejiang Province Science and Technology Plan Research and Xinmiao Talent Program (2020R413035 to HYZ), Wenzhou Medical University (QTJ16006 to FH).

Disclosure: **H. Zheng,** None; **X. Ying,** None; **X. He,** None; **J. Qu,** None; **F. Hou,** None

References

1. Holden BA, Fricke TR, Wilson DA, et al. Global Prevalence of Myopia and High Myopia and Temporal Trends from 2000 through 2050. *Ophthalmology*. 2016;123:1036–1042.
2. Morgan IG, Ohno-Matsui K, Saw SM. Myopia. *Lancet*. 2012;379:1739–1748.
3. Morgan IG, French AN, Ashby RS, et al. The epidemics of myopia: Aetiology and prevention. *Prog Retin Eye Res*. 2018;62:134–149.
4. Atchison DA, Jones CE, Schmid KL, et al. Eye shape in emmetropia and myopia. *Invest Ophthalmol Vis Sci*. 2004;45:3380–3386.
5. Chui TY, Yap MK, Chan HH, Thibos LN. Retinal stretching limits peripheral visual acuity in myopia. *Vision Res*. 2005;45:593–605.
6. Liou SW, Chiu CJ. Myopia and contrast sensitivity function. *Curr Eye Res*. 2001;22:81–84.
7. Chen JC, Brown B, Schmid KL. Delayed mfERG responses in myopia. *Vision Res*. 2006;46:1221–1229.
8. Itakura H, Kishi S, Li D, Nitta K, Akiyama H. Vitreous changes in high myopia observed by swept-source

optical coherence tomography. *Invest Ophthalmol Vis Sci*. 2014;55:1447–1452.
9. Moghadas Sharif N, Shoeibi N, Ehsaei A, Atchison D. Structure versus function in high myopia using optical coherence tomography and automated perimetry. *Clin Exp Optom*. 2019;102:335–340.
10. Wolsley CJ, Saunders KJ, Silvestri G, Anderson RS. Investigation of changes in the myopic retina using multifocal electroretinograms, optical coherence tomography and peripheral resolution acuity. *Vision Res*. 2008;48:1554–1561.
11. Collins JW, Carney LG. Visual performance in high myopia. *Curr Eye Res*. 1990;9:217–223.
12. Atchison DA, Schmid KL, Pritchard N. Neural and optical limits to visual performance in myopia. *Vision Res*. 2006;46:3707–3722.
13. Fledelius HC, Jacobsen N, Li XQ, Goldschmidt E. The Longitudinal Danish High Myopia Study, Cohort 1948: at age 66 years visual ability is only occasionally affected by visual field defects. *Acta Ophthalmol*. 2019;97:36–43.
14. Stoimenova BD. The effect of myopia on contrast thresholds. *Invest Ophthalmol Vis Sci*. 2007;48:2371–2374.
15. Kawabata H, Adachi-Usami E. Multifocal electroretinogram in myopia. *Invest Ophthalmol Vis Sci*. 1997;38:2844–2851.
16. Taylor CP, Shepard TG, Rucker FJ, Eskew RT, Jr. Sensitivity to S-Cone Stimuli and the Development of Myopia. *Invest Ophthalmol Vis Sci*. 2018;59:4622–4630.
17. Wutz A, Melcher D. The temporal window of individuation limits visual capacity. *Front Psychol*. 2014;5:952.
18. Di Lollo V. Temporal integration in visual memory. *J Exp Psychol Gen*. 1980;109:75–97.
19. Wutz A, Melcher D. Temporal buffering and visual capacity: the time course of object formation underlies capacity limits in visual cognition. *Atten Percept Psychophys*. 2013;75:921–933.
20. Zimmermann E, Morrone MC, Burr DC. Spatial position information accumulates steadily over time. *J Neurosci*. 2013;33:18396–18401.
21. Kuo HY, Schmid KL, Atchison DA. Visual backward masking performance in young adult emmetropes and myopes. *Optom Vis Sci*. 2012;89:E90–E96.
22. Kuo H-Y, Atchison DA, Schmid KL. Dot motion perception in young adult emmetropes and myopes. *Optometry Vision Sci*. 2018;95:498–504.
23. Vera-Diaz FA, Bex PJ, Ferreira A, Kosovicheva A. Binocular temporal visual processing in myopia. *J Vis*. 2018;18:17.
24. Breitmeyer BG, Öğmen H. *Visual masking: Time slices through conscious and unconscious vision,* 2nd ed. New York, NY, US: Oxford University Press; 2006;xi:370-xi, 370.
25. Bachmann T, Francis G. Visual Masking: Studying Perception, Attention, and Consciousness. In: Bachmann T, Francis G . (eds), *Visual Masking*. San Diego: Academic Press; 2014;1–108.
26. Schneider BA, Avivi-Reich M, Mozuraitis M. A cautionary note on the use of the analysis of covariance (ANCOVA) in classification designs with and without within-subject factors. *Front Psychol*. 2015;6:474.
27. Liu X, Shen M, Yuan Y, et al. Macular Thickness Profiles of Intraretinal Layers in Myopia Evaluated by Ultrahigh-Resolution Optical Coherence Tomography. *Am J Ophthalmol*. 2015;160:53–61.e52.
28. Lu ZL, Jeon ST, Dosher BA. Temporal tuning characteristics of the perceptual template and endogenous cuing of spatial attention. *Vision Res*. 2004;44:1333–1350.
29. He X, Shen M, Cui R, et al. The Temporal Window of Visual Processing in Aging. *Invest Ophthalmol Vis Sci*. 2020;61:60.
30. Kleiner M, Brainard D, Pelli D, et al. What's new in Psychtoolbox-3. *Cognitive Computational Psychophys*. 2007;36:1–89.
31. Seijas O, Gómez de Liaño P, Gómez de Liaño R, et al. Ocular dominance diagnosis and its influence in monovision. *Am J Ophthalmol*. 2007;144:209–216.
32. Georgeson MA. Temporal properties of spatial contrast vision. *Vision Res*. 1987;27:765–780.
33. Koenderink JJ, van Doorn AJ. Dual percept of movement and spatial periodicity in stroboscopically illuminated moving noise patterns. *J Opt Soc Am*. 1980;70:456–460.
34. Watson AB, Ahumada AJ, Farrell JE. Window of visibility: a psychophysical theory of fidelity in time-sampled visual motion displays. *J Opt Soc Am A*. 1986;3:300–307.
35. Kontsevich LL, Tyler CW. Bayesian adaptive estimation of psychometric slope and threshold. *Vision Res*. 1999;39:2729–2737.
36. Watson AB. Probability summation over time. *Vision Res*. 1979;19:515–522.
37. Lesmes LA, Jeon ST, Lu ZL, Dosher BA. Bayesian adaptive estimation of threshold versus contrast external noise functions: the quick TvC method. *Vision Res*. 2006;46:3160–3176.
38. Lu ZL, Dosher BA. Characterizing human perceptual inefficiencies with equivalent internal noise. *J Opt Soc Am A Opt Image Sci Vis*. 1999;16:764–778.
39. Lu ZL, Dosher BA. Characterizing observers using external noise and observer models: assessing internal representations with external noise. *Psychol Rev*. 2008;115:44–82.
40. Wutz A, Melcher D. The temporal window of individuation limits visual capacity. *Frontiers in psychology*. 2014;5:952.
41. McKeeff TJ, Remus DA, Tong F. Temporal limitations in object processing across the human ventral visual pathway. *J Neurophysiol*. 2007;98:382–393.
42. Landau Ayelet N, Fries P. Attention Samples Stimuli Rhythmically. *Current Biology*. 2012;22:1000–1004.
43. VanRullen R, Koch C. Is perception discrete or continuous? *Trends Cogn Sci*. 2003;7:207–213.
44. Wang Y, Ye J, Shen M, et al. Photoreceptor Degeneration is Correlated With the Deterioration of Macular Retinal Sensitivity in High Myopia. *Invest Ophthalmol Vis Sci*. 2019;60:2800–2810.
45. Lee MW, Nam KY, Park HJ, Lim HB, Kim JY. Longitudinal changes in the ganglion cell-inner plexiform layer thickness in high myopia: a prospective observational study. *Br J Ophthalmol*. 2019;104:604–609.
46. Park S, Kim SH, Park TK, Ohn YH. Evaluation of structural and functional changes in non-pathologic myopic fundus using multifocal electroretinogram and optical coherence tomography. *Doc Ophthalmol*. 2013;126:199–210.
47. Mäntyjärvi M, Tuppurainen K. Colour vision and dark adaptation in high myopia without central retinal degeneration. *Br J Ophthalmol*. 1995;79:105–108.
48. Ye J, Shen M, Huang S, et al. Visual Acuity in Pathological Myopia Is Correlated With the Photoreceptor Myoid and Ellipsoid Zone Thickness and Affected by Choroid Thickness. *Invest Ophthalmol Vis Sci*. 2019;60:1714–1723.
49. Wang P, Xiao X, Huang L, Guo X, Zhang Q. Cone-rod dysfunction is a sign of early-onset high myopia. *Optom Vis Sci*. 2013;90:1327–1330.
50. Kader MA. Electrophysiological study of myopia. *Saudi J Ophthalmol*. 2012;26:91–99.
51. Wang Y, Bensaid N, Tiruveedhula P, et al. Human foveal cone photoreceptor topography and its dependence on eye length. *Elife*. 2019;8.
52. Turatto M, Facoetti A, Serra G, et al. Visuospatial attention in myopia. *Brain Res Cogn Brain Res*. 1999;8:369–372.
53. Kang MT, Wang B, Li S, et al. Attention-Related-Functional Changes Induced By Imposed Myopia Defocus From Spectacle Lens. *Invest Ophthalmol Vis Sci*. 2017;58:2741–2741.
54. Zhai L, Li Q, Wang T, et al. Altered functional connectivity density in high myopia. *Behav Brain Res*. 2016;303:85–92.

Investigative Ophthalmology & Visual Science

55. Huang X, Zhou FQ, Hu YX, et al. Altered spontaneous brain activity pattern in patients with high myopia using amplitude of low-frequency fluctuation: a resting-state fMRI study. *Neuropsychiatr Dis Treat*. 2016;12:2949–2956.
56. Himmelberg MM, Wade AR. Eccentricity-dependent temporal contrast tuning in human visual cortex measured with fMRI. *Neuroimage*. 2019;184:462–474.
57. Livingstone M, Hubel D. Segregation of form, color, movement, and depth: anatomy, physiology, and perception. *Science*. 1988;240:740–749.
58. Hartmann E, Lachenmayr B, Brettel H. The peripheral critical flicker frequency. *Vision Res*. 1979;19:1019–1023.
59. McKee SP, Taylor DG. Discrimination of time: comparison of foveal and peripheral sensitivity. *J Opt Soc Am A*. 1984;1:620–627.
60. Snowden RJ, Hess RF. Temporal frequency filters in the human peripheral visual field. *Vision Res*. 1992;32:61–72.
61. Liu HH, Xu L, Wang YX, et al. Prevalence and progression of myopic retinopathy in Chinese adults: the Beijing Eye Study. *Ophthalmology*. 2010;117:1763–1768.
62. Kerber KL, Thorn F, Bex PJ, Vera-Diaz FA. Peripheral contrast sensitivity and attention in myopia. *Vision Res*. 2016;125:49–54.
63. Macedo A, Encarnação TJ, Vilarinho D, Baptista AG. An exploratory study of temporal integration in the peripheral retina of myopes. *Adv. Opt. Photonics*. 2017;10453:104532G.
64. Hacker MJ, Ratcliff R. A revised table of d' for M-alternative forced choice. *Percept Psychophys*. 1979;26:168–170.
65. Hou F, Lu ZL, Huang CB. The external noise normalized gain profile of spatial vision. *J Vis*. 2014;14:9.

Appendix A: The Elaborated Perceptual Template Model (ePTM)

The ePTM, developed by Lu et al.[28] has been used previously to investigate the effect of attention and aging[29] on the temporal processing. It consists of an additive internal noise source, a multiplicative noise source, a nonlinear transducer function, a perceptual template and a decision unit. The visual information stream consists of both signal and external noises, that enters the visual system through a perceptual template. The perceptual template is essentially a spatiotemporal filter with a total gain value of β to the signal relative to the external noise, and weight W_t at different time t, which can selectively pick up task-relevant information and exclude task-irrelevant information. After filtering, the information goes through a non-linear transducer, characterized by a power function with an exponent of γ, then gets contaminated by an internal additive noise Na and multiplicative noise Nm, which mimics the contrast-gain control mechanism of neurons and finally is sent to the decision unit. A schematic diagram of the ePTM is shown in Figure 2.

We assign the temporal weight W_t for each stimulus frame (from −8 to 8 frames relative to the stimuli onset) so that we can estimate the entire shape of the template over time (Fig. 1b). As the total gain of the perceptual template to external noise is normalized to 1.0 in the PTM,[38] we have the following:

$$\sum_{t=-8}^{8} W_t^2 = 1. \tag{A1}$$

Recall that we have four different external noise configurations, corresponding to ±1, ±2, ±3 & 4, and ±5,6,7 & 8 image frame positions symmetrically distributed around the signal frame 0. There were two, two, four, and eight frames in SOA 16.7 ms, 33.3 ms, 50.0 ms, and 83.3 ms conditions, respectively. It essentially allowed us to obtain the average weight for the multi-frame external noise conditions:

$$W_t = \begin{cases} W_{16.7}, & if \quad t = -1, 1, \\ W_{33.4}, & if \quad t = -2, 2, \\ W_{50.0}, & if \quad t = -4, -3, 3, 4, \\ W_{83.4}, & if \quad t = -8, -7, -6, -5, 5, 6, 7, 8. \end{cases} \tag{A2}$$

So $W_{16.7}$, $W_{33.4}$, $W_{50.0}$, and $W_{83.4}$ are to be optimized during model fitting process.

Assume the signal is represented by the contrast c. For external noise images each with variance σ^2, the total variance of external noise in a given temporal configuration is summed over the entire stimuli duration:

$$N_{ext}^2 = \sum_{t=-8}^{8} (W_t \sigma_t)^2, \tag{A3}$$

where t is the time in the unit of frame from −8 to 8, $\sigma_t = \sigma$, when the noise presents, and $\sigma_t = 0$, when the blank frame presents (Fig. 1a). Combining the Equation (A2) and the Equation (A3), we have

$$N_{ext}^2 = \begin{cases} 2\left(W_{16.7}\sigma\right)^2, & if \quad SOA = 16.7ms, \\ 2(W_{33.4}\sigma)^2, & if \quad SOA = 33.4ms, \\ 4(W_{50.0}\sigma)^2, & if \quad SOA = 50.0ms, \\ 8(W_{83.4}\sigma)^2, & if \quad SOA = 83.4ms. \end{cases} \tag{A4}$$

The noise duration in the number of frames in each condition was used in the calculation of noise. And the sensitivity of observer can be written as

$$d' = \frac{(\beta c)^\gamma}{\sqrt{\left((\beta c)^{2\gamma} + N_{ext}^{2\gamma}\right) Nm^2 + Na^2}}, \tag{A5}$$

where the numerator represents the total signal strength in the system, and the denominator represents the total noise after combining all the internal and external noise sources.

Then, the percent correct psychometric function of the observer can be derived from the d' psychometric function[64]:

$$P(c) = \int_{-\infty}^{+\infty} \phi\left(x - d'(c)\right) \Phi(x)\, dx, \qquad \text{(A6)}$$

where c represents the contrast of the signal, x is the variable of integration in the d' space, $\varphi()$ is the probability density function of the standard distribution, and $\Phi()$ represents the cumulative probability density functions of the standard distribution, respectively.

In our experiment, the same eye of each participant was tested at both fovea and periphery. According to previous research,[28,65] multiplicative noise Nm or nonlinear transducer γ of same observer normally does not change across different conditions. So we constructed a combined ePTM to account for the behavioral data at fovea and periphery at the same time. The combined ePTM assumes that the fovea and the periphery have their own set of Na, β, and temporal weights W_t, but share same Nm, and γ. This leaves the model a total of 12 free parameters, two Na, two β, one Nm, one γ, one set of $W_{16.7}$, $W_{33.3}$, $W_{50.0}$ for the fovea, and another set of $W_{16.7}$, $W_{33.3}$, $W_{50.0}$ for the periphery.

Finally, equation A6 was used to fit the raw trial-by-trial response data.

Investigative Ophthalmology & Visual Science